AIAA 81-4324

Splice Joint Containing a Crack Along the Fastener Line

J.T.S. Wang*
Georgia Institute of Technology, Atlanta, Ga.
and
C. S. Chu,† O. L. Freyre,‡ and T. M. Hsu§
Lockheed-Georgia Company, Marietta, Ga.

This paper describes the analysis procedure for determining displacements and stresses in a splice joint containing a panel crack along the fastener line. The presented analytical solutions based on the linear elasticity theory satisfy all boundary conditions except along the crack-line where a collocation procedure is used. Results obtained from the general analysis, together with a high order crack-tip element, are used to determine crack-tip stress-intensity levels. Results for a joint without a crack is first examined for the convergence of the general solution, and rapid convergence is observed. Numerical results for two examples containing a crack are presented, and convergence of solutions based on the numerical results is discussed for illustrative purposes.

Nomenclature

a	= half crack length
b	= half of the panel width
d	= fastener diameter
E	= modulus of elasticity
f_t	= applied far-field stress
F	= Airy stress function
G	= shear modulus of elasticity
J	= number of fasteners
K_I	= stress intensity factor
N_a	= $2N$ = applied far-field stress resultant
N_x, N_y, N_{xy}	= stress resultants
P_i	= fastener shear load in longitudinal direction
Q_i	= fastener shear load in transverse direction
t	= thickness
u, v	= displacement components
x, y	= Cartesian coordinates
$\epsilon_x, \epsilon_y, \gamma_{xy}$	= strain components
$\sigma_x, \sigma_y, \tau_{xy}$	= stress components
ν	= Poisson's ratio
λ	= normalized stress intensity factor

Introduction

CRACKS often occur along fastener lines of a spliced joint. When a crack occurs, it is important to know the extent of change in fastener loads, local stress levels, as well as crack-tip stress-intensity factors corresponding to various crack lengths so that the damage tolerance capability of the structure can be established. Since it is generally impossible to obtain exact solutions for cracked structures, many structures containing cracks are analyzed by numerical procedures, such as the finite-element method. While these numerical procedures are effective, they are generally time consuming and expensive. Other analytical procedures will be more desirable if they can be developed effectively. In this respect, Wang and Hsu[1] analyzed a partially cracked panel by applying a boundary collocation procedure along the crack-line. Results indicated that the analysis was suitable and effective in computing stresses and deformations with a high degree of accuracy at all locations except in the immediate vicinity of the crack tip. These findings motivated the authors to analyze the present problem based on plane elasticity theory using series solutions in conjunction with a collocation procedure along the fastener line containing a crack. Displacements generated from this analysis will provide the boundary conditions for a crack-tip element which permits a direct and accurate determination of stress intensity factors.

General analysis concepts and some preliminary results were presented at the Fifth Canadian Congress of Applied Mechanics.[2] Included in the present paper is a complete discussion of the formulation and analysis of the stress distribution and deformation of a splice-joint containing a crack subjected to loads in the direction perpendicular to the crack. The joint configuration is idealized by considering the geometry at the splice to be symmetrical about the midline of splice plates and about the midplane of the main sheet. In addition, the supporting frame at the splice location is considered to be rigid, resulting in zero displacements along the midline of the splice plates. Fastener loads are developed through pins of infinite rigidity and zero diameter. It is recognized that the flexibility of the fastener will have an influence on stress intensity at the crack tip. The influence of fastener flexibility in these types of problems was addressed in Refs. 3-6 in which the flexibility is characterized by an idealized linear spring or by a load-deflection relation based on test results. If such idealized representation of fastener flexibility is used, the present analysis can be extended easily to incorporate the effect of fastener flexibility when maintaining continuity of displacements of the main sheet and the splice plates at fastener locations. The zero diameter consideration may represent an idealized spot weld. Otherwise fastener hole effects on the stress intensity of cracks emanating from a hole may be considered by applying a correction factor based on the analysis of Bowie.[7] However, exact account of the effect of the hole is beyond the present scope of study.

Analysis

Due to symmetry in geometry and loading, only one quarter of the joint needs to be analyzed. The geometry and some symbols for the joint having one row of equally spaced fasteners are shown in Figs. 1 and 2. The area is divided further into four separate regions designated as regions 1-4 as shown in Fig. 2. The far-field applied stress resultant $N_a = 2N$ in the main sheet is distributed uniformly and the main sheet is considered to be infinitely wide when compared to the length of the crack. A plane state of stress is assumed for each region and linear elastic theory is followed. Fastener shear

Received Feb. 4, 1980; revision received April 21, 1981.

*Professor, School of Engineering Science and Mechanics; also, Consultant Lockheed Georgia Company, Marietta, Ga.

†Aircraft Development Engineer, Specialist, Advanced Structures Department.

‡Scientist, Advanced Structures Department.

§Aircraft Development Engineer, Specialist, Advanced Structures Department. Member AIAA.

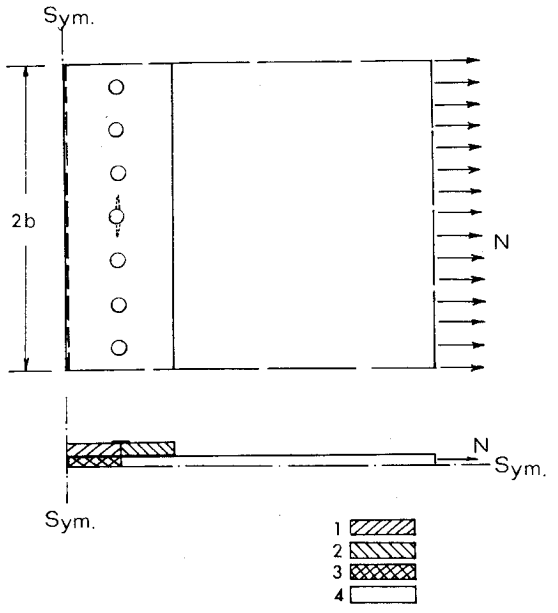

Fig. 1 Geometry.

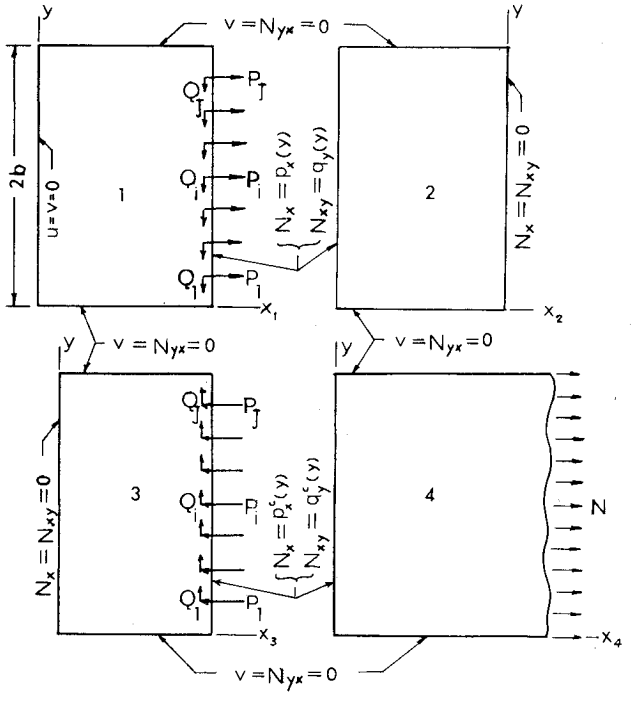

Fig. 2 Loading and boundary conditions.

force components P_i and Q_i in the longitudinal and transverse directions, respectively, will be considered as concentrated external loads on regions 1 and 3. It is clear that if there is no crack, stresses and displacements will vary periodically in the y direction with transverse displacement v and shearing stress τ_{yx} equal to zero along each midline between two adjacent fasteners. Furthermore, the load component Q_i in the transverse y direction in all fasteners must be zero. Inasmuch as the effect of cracks on stresses and deformation is known to be localized in nature, the periodical phenomenon will recover at areas sufficiently distant from the crack. Consequently, each longitudinal edge of the joint is selected along a midline between two adjacent fasteners at some distance from the crack. While the boundary conditions $v=\tau_{yx}=0$ along the edges $y=0$ and $2b$ will be specified, the values of Q in the fasteners located immediately next to these edges will be examined in order to verify the adequacy of the panel width used in the analysis. Although the theory and equations relating to linear elasticity can be found in standard textbooks such as Refs. 8-10, the pertinent equations that applied to the four regions are included in the paper for clarity. The equilibrium equations are

$$\frac{\partial N_x}{\partial x}+\frac{\partial N_{yx}}{\partial y}=0 \tag{1}$$

$$\frac{\partial N_{xy}}{\partial x}+\frac{\partial N_y}{\partial y}=0 \tag{2}$$

where N_x, N_y, and N_{xy} are stress resultants. Introducing the Airy stress function F such that

$$N_x = t\sigma_x = \frac{\partial^2 F}{\partial y^2} \tag{3}$$

$$N_y = t\sigma_y = \frac{\partial^2 F}{\partial x^2} \tag{4}$$

$$N_{xy} = t\tau_{xy} = -\frac{\partial^2 F}{\partial x \partial y} \tag{5}$$

where σ_x, σ_y, and τ_{xy} are stresses and t the thickness. The Airy stress function is governed by

$$\nabla^4 F = 0 \tag{6}$$

The stress, strain, and displacement relations are

$$\epsilon_x = \frac{\partial u}{\partial x} = \frac{1}{Et}(N_x - \nu N_y) \tag{7}$$

$$\epsilon_y = \frac{\partial v}{\partial y} = \frac{1}{Et}(N_y - \nu N_x) \tag{8}$$

$$\gamma_{xy} = \frac{\partial u}{\partial y}+\frac{\partial v}{\partial x} = \frac{1}{Gt}N_{xy} \tag{9}$$

$$N_x = [Et/(1-\nu^2)](\epsilon_x + \nu\epsilon_y) \tag{10}$$

$$N_y = [Et/(1-\nu^2)](\epsilon_y + \nu\epsilon_x) \tag{11}$$

$$N_{xy} = = Gt\gamma_{xy} \tag{12}$$

in which E is the modulus of elasticity, ν the Poisson's ratio and G the shear rigidity. Substituting Eqs. (10-12) into Eqs. (1) and (2), one obtains

$$\frac{\partial^2 u}{\partial x^2}+\frac{1+\nu}{2}\frac{\partial^2 v}{\partial x \partial y}+\frac{1-\nu}{2}\frac{\partial^2 u}{\partial y^2}=0 \tag{13}$$

$$\frac{1+\nu}{2}\frac{\partial^2 u}{\partial x \partial y}+\frac{1-\nu}{2}\frac{\partial^2 v}{\partial x^2}+\frac{\partial^2 v}{\partial y^2}=0 \tag{14}$$

The boundary conditions along $y=0$ and $2b$ are

$$\tau_{xy}=0 \tag{15}$$

and

$$v=0 \tag{16}$$

The general solution of Eq. (6) satisfying condition Eq. (15) will be taken in the following form:

$$F=\sum_{m=0}^{\infty} F_m(x)\cos\alpha_m y+\frac{1}{2}Ay^2 \tag{17}$$

where $\alpha_m = m\pi/2b$ and A is a constant. In addition, the general solutions of F_m satisfying Eq. (6) are

$$F_0 = \sum_{j=1}^{2} B_{0j} x^{j+1} \tag{18}$$

$$F_m = \sum_{j=1}^{4} B_{mj} f_{mj} \tag{19}$$

in which

$$f_{m1} = \cosh\alpha_m x \tag{20}$$

$$f_{m2} = \sinh\alpha_m x \tag{21}$$

$$f_{m3} = \alpha_m x \cosh\alpha_m x \tag{22}$$

$$f_{m4} = \alpha_m x \sinh\alpha_m x \tag{23}$$

The far-field applied stress in region 4 of the main sheet is at sufficient distance away from the fastener line, that the simpler solution

$$F_m = B_{m1} e^{-\alpha_m x} + B_{m2} \alpha_m x e^{-\alpha_m x} \tag{24}$$

which is valid near the fastener line may be used.

Substituting Eqs. (3-5) in conjunction with Eqs. (18), (19), or (24) into Eqs. (7-9), one obtains

$$Etu = -\sum_{m=1}^{\infty} \left(\alpha_m^2 \int F_m dx + \nu \frac{dF_m}{dx}\right) \cos\alpha_m y + [A - \nu(3B_{02}x + 2B_{01})]x + u_0(y) \tag{25}$$

and

$$Etv = \sum_{m=1}^{\infty} \frac{1}{\alpha_m} \left(\frac{d^2 F_m}{dx^2} + \nu\alpha_m^2 F_m\right) \sin\alpha_m y + (6B_{02}x + 2B_{01} - \nu A)y + v_0(x) \tag{26}$$

To satisfy conditions Eq. (16), one concludes that

$$v_0(x) = 0 \tag{27}$$

$$B_{02} = 0 \tag{28}$$

and

$$2B_{01} = \nu A \tag{29}$$

Substituting Eqs. (25) and (26) in conjunction with Eqs. (28) and (29) into Eqs. (13) and (14) and then integrating with respect to y, gives

$$du_0/dy = C \tag{30}$$

where C is the integration constant. To satisfy conditions given in Eq. (15), one concludes that $C = 0$; and, as a result,

$$u_0 = \text{const} \tag{31}$$

Now the displacements are represented completely in terms of F_m. From Eqs. (3-5) in conjunction with Eqs. (18), (28), and (29), the expressions for stress resultants in terms of F_m are given as follows.

$$N_x = -\sum_{m=1}^{\infty} \alpha_m^2 F_m \cos\alpha_m y + A \tag{32}$$

$$N_y = \sum_{m=1}^{\infty} \frac{d^2 F_m}{dx^2} \cos\alpha_m y + \nu A \tag{33}$$

$$N_{xy} = \sum_{m=1}^{\infty} \alpha_m \frac{dF_m}{dx} \sin\alpha_m y \tag{34}$$

Clearly, the constant A for each region given in Eq. (32) represents the average value of N_x for that region. Consequently,

$$A = 0 \quad \text{for regions 2 and 3} \tag{35}$$

and

$$A = N \quad \text{for regions 1 and 4} \tag{36}$$

where N is the uniformly applied stress resultant. The x-coordinate for regions 1,2, and 3 designated by x_1, x_2, and x_3 is measured from the edges without fasteners as shown in Fig. 2, and the lengths of these regions are $\bar{x}_1$, $\bar{x}_2$, and $\bar{x}_3$, respectively. The y-axis for region 4 of the main sheet is located along the fastener line. The interacting stresses in this plane between adjacent regions are represented by Fourier series with unknown coefficients. The remaining boundary conditions for all four regions can now be listed separately as follows.

Region 1

$$u(0,y) = v(0,y) = 0 \tag{37}$$

$$N_x(\bar{x}_1, y) = N + \sum_{m=1}^{\infty} \left(\frac{1}{b} \sum_{i=1}^{J} P_i \cos\alpha_m y_i + p_m\right) \cos\alpha_m y \tag{38}$$

$$N_{xy}(\bar{x}_1, y) = \sum_{m=1}^{\infty} \left(\frac{1}{b} \sum_{i=1}^{J} Q_i \sin\alpha_m y_i + q_m\right) \sin\alpha_m y \tag{39}$$

Region 2

$$N_x(0,y) = N_{xy}(0,y) = 0 \tag{40}$$

$$N_x(-\bar{x}_2, y) = \sum_{m=1}^{\infty} p_m \cos\alpha_m y \tag{41}$$

$$N_{xy}(-\bar{x}_2, y) = \sum_{m=1}^{\infty} q_m \sin\alpha_m y \tag{42}$$

Region 3

$$N_x(0,y) = N_{xy}(0,y) = 0 \tag{43}$$

$$N_x(\bar{x}_3, y) = \sum_{m=1}^{\infty} \left(-\sum_{i=1}^{J} \frac{1}{b} P_i \cos\alpha_m y_i + p_m^c\right) \cos\alpha_m y \tag{44}$$

$$N_{xy}(\bar{x}_3, y) = \sum_{m=1}^{\infty} \left(-\sum_{i=1}^{J} \frac{1}{b} Q_i \sin\alpha_m y_i + q_m^c\right) \sin\alpha_m y \tag{45}$$

Region 4

$$N_x(0,y) = N + \sum_{m=1}^{\infty} p_m^c \cos\alpha_m y \tag{46}$$

$$N_{xy}(0,y) = \sum_{m=1}^{\infty} q_m^c \sin\alpha_m y \tag{47}$$

in which p_m, q_m, p_m^c, and q_m^c are unknown Fourier coefficients of interacting stresses, and J is the number of fasteners in the splice. Satisfying conditions along $x_i = 0$ results in

$$u_0^{(1)} = 0, \quad B_{m4}^{(1)} = -\frac{1+\nu}{2} B_{m1}^{(1)}, \quad B_{m2}^{(1)} = \frac{1-\nu}{1+\nu} B_{m3}^{(1)}$$

$$B_{m1}^{(2)} = 0, \quad B_{m2}^{(2)} = -B_{m3}^{(2)}, \quad B_{m1}^{(3)} = 0, \quad B_{m2}^{(3)} = -B_{m3}^{(3)}$$

$$B_{m1}^{(4)} = -\frac{p_m^c}{\alpha_m^2}, \quad B_{m2}^{(4)} = \frac{1}{\alpha_m^2}(q_m^c - p_m^c) \tag{48}$$

where the superscript in parentheses denotes the region number. Furthermore, by satisfying the stress boundary condition along the fastener lines for regions 1, 2, and 3, one can express all constants $B_{mi}^{(i)}$ in terms of unknown Fourier coefficients p_m, q_m, p_m^c, and q_m^c. These coefficients together with P_i, Q_i, and u_0 for regions 2, 3, and 4 are the remaining unknown quantities which must be determined.

By satisfying the continuity conditions along the fastener line between regions 1 and 2,

$$u^{(1)}(\bar{x}_1,y) = u^{(2)}(-\bar{x}_2,y) \tag{49}$$

$$v^{(1)}(\bar{x}_1,y) = v^{(2)}(-\bar{x}_2,y) \tag{50}$$

Using Eqs. (25), (26), and related results, one obtains

$$u_0^{(2)} = \frac{1-\nu^2}{2b}\bar{x}_1 \sum_{i=1}^{J} P_i \tag{51}$$

$$\begin{Bmatrix} p_m \\ q_m \end{Bmatrix} = \begin{bmatrix} D_{11} & D_{12} \\ D_{21} & D_{22} \end{bmatrix} \sum_{i=1}^{J} \begin{Bmatrix} P_i \cos\alpha_m y_i \\ Q_i \sin\alpha_m y_i \end{Bmatrix} \tag{52}$$

in which the detailed expressions for the constants D_{11}, D_{12}, D_{21}, and D_{22} are omitted. Clearly, the displacements at the fastener locations of the splice plate can be expressed in terms of fastener loads in the following general form

$$E_s t_s u_{sj} = \sum_{i=1}^{J} (\beta_{ji}P_i + \beta_{ji}^* Q_i) + \frac{1-\nu^2}{2b}\bar{x}_1 \sum_{i=1}^{J} P_i \tag{53}$$

$$E_s t_s v_{sj} = \sum_{i=1}^{J} (\lambda_{ji}P_i + \lambda_{ji}^* Q_i) \tag{54}$$

in which β_{ji}, β_{ji}^*, λ_{ji}, and λ_{ji}^* are constants, the subscript s denotes splice plate, and $j = 1, 2, \ldots, J$ identifies the fastener locations.

The displacements along the fastener line of regions 3 and 4 may be represented in the following general forms.

$$E_c t_c u^{(3)} = \sum_{m=1}^{\infty} (G_m^{(3)} p_m^c + H_m^{(3)} q_m^c)\cos\alpha_m y + u_0^{(3)} \tag{55}$$

$$E_c t_c v^{(3)} = \sum_{m=1}^{\infty} (J_m^{(3)} p_m^c + K_m^{(3)} q_m^c)\sin\alpha_m y \tag{56}$$

$$E_c t_c u^{(4)} = \sum_{m=1}^{\infty} (G_m^{(4)} p_m^c + H_m^{(4)} q_m^c)\cos\alpha_m y + N(1-\nu^2)x_4 + u_0^{(4)} \tag{57}$$

$$E_c t_c v^{(4)} = \sum_{m=1}^{\infty} (J_m^{(4)} p_m^c + K_m^{(4)} q_m^c)\sin\alpha_m y \tag{58}$$

in which $G_m^{(i)}$, $H_m^{(i)}$, $J_m^{(i)}$, and $K_m^{(i)}$ for $i = 3$ and 4 are constants, and the subscript c denotes the main sheet. Using Eqs. (53-56) to maintain continuity in displacements between the splice plate and the main plate at the fastener locations, one obtains for $j = 1, 2, \ldots J$ the following equations.

$$\sum_{m=1}^{\infty} (C_{jm}p_m^c + E_{jm}q_m^c) + \sum_{i=1}^{J} (\Delta_{ji}P_i + \zeta_{ji}Q_i) = -\frac{E_c t_c}{2E_s t_s}(1-\nu^2)N\bar{x}_1 + U_0^{(3)} \tag{59}$$

$$\sum_{m=1}^{\infty} (C_{jm}^* p_m^c + E_{jm}^* q_m^c) + \sum_{i=1}^{J} (\Delta_{ji}^* P_i + \zeta_{ji}^* Q_i) = 0 \tag{60}$$

in which all the coefficients are known. The unknown constant value of $u_0^{(3)}$ in Eq. (59) may be determined from Eq. (59) by taking j to be any integer between 1 and J. In the present analysis $j = 1$ is used. As a result, Eq. (59) becomes

$$\sum_{m=1}^{\infty} [(C_{km} - C_{1m})p_m^c + (E_{km} - E_{1m})q_m^c] + \sum_{i=1}^{J} [(\Delta_{ki} - \Delta_{1i})P_i + (\zeta_{ki} - \zeta_{1i})Q_i] = 0 \tag{61}$$

for $k = 2, 3, \ldots, J$, and

$$u_0^{(3)} = \sum_{m=1}^{\infty} (C_{1m}p_m^c + E_{1m}q_m^c) + \sum_{i=1}^{J} (\Delta_{1i}P_i + \zeta_{1i}Q_i) + \frac{E_c t_c}{2E_s t_s}(1-\nu^2)N\bar{x}_1 \tag{62}$$

By equating Eqs. (53) and (57) at $x_4 = 0$ and for $j = 1$, one obtains

$$u_0^{(4)} = \sum_{m=1}^{\infty} \frac{1}{\alpha_m}\cos\alpha_m y_1 [2p_m^c - (1-\nu)q_m^c] + \frac{E_c t_c}{E_s t_s} \sum_{i=1}^{J} [(\beta_{1i}P_i + \beta_{1i}^* Q_i) + \frac{1-\nu^2}{2b}\bar{x}_1 P_i] \tag{63}$$

Now all stresses and displacements along the fastener line of regions 3 and 4 can be expressed in terms of p_m^c, q_m^c, P_i, and Q_i. The continuity conditions along the fastener line of the main sheet

$$u^{(3)}(\bar{x}_3,y) = u^{(4)}(0,y) \tag{64}$$

$$v^{(3)}(\bar{x}_3,y) = v^{(4)}(0,y) \tag{65}$$

must be satisfied for the uncracked region of y except at the first fastener location ($y_j = y_1$) where these conditions have already been satisfied. Along the cracked region, the conditions $N_x = N_{xy} = 0$ must also be satisfied and result in

$$\sum_{m=1}^{\infty} p_m^c \cos\alpha_m y = -N \tag{66}$$

$$\sum_{m=1}^{\infty} q_m^c \sin\alpha_m y = 0 \tag{67}$$

Finally, the satisfaction of the overall equilibrium condition yields

$$\sum_{i=1}^{J} P_i = 2bN \tag{68}$$

Conditions given in Eqs. (64-67) in conjunction with Eq. (68) are satisfied by using a collocation procedure which results in a system of simultaneous algebraic equations for the fastener loads P_i and Q_i, and for a finite number of Fourier coefficients p_m^c and q_m^c. Upon solving these equations, the Fourier coefficients p_m and q_m can be determined from Eq. (52). Consequently, the stresses and displacements in all four regions can be computed. Rapid convergence of solutions was observed in a number of cases investigated. It is clear that the convergence on stresses along the fastener line particularly near the fastener and crack locations would be much slower than those in regions sufficiently away from these areas. While the stresses in the immediate vicinity of the fastener line and the crack may converge slowly, the displacements have been shown to be well behaved. In the example problems

Table 1 Normalized σ_x along $x=0.2b$

	No. of terms		
y/b	5	8	10
0	0.97	1.01	1.00
0.2	1.04	1.01	1.01
0.4	1.01	1.03	1.03
0.6	1.14	1.11	1.12
0.8	0.90	1.50	1.51
1.0	2.58	2.68	2.70

Table 2 Normalized σ_x and u along $x=0$

	Stress No. of terms		Displacement No. of terms	
y/b	8	10	8	10
0	1.00	1.00	1.05	1.00
0.2	0.91	1.01	1.04	1.00
0.4	0.66	1.02	1.02	0.99
0.6	3.58	1.03	0.99	0.96
0.8	1.13	1.04	0.92	0.90
1.0	5.10	6.12	0.67	0.65

Table 3 Normalized σ_x along $x=0.08b$

	No. of terms		
y/b	30	35	40
0	1.00	1.01	1.00
0.08	1.07	1.07	1.07
0.16	1.52	1.54	1.53
0.24	1.52	1.54	1.53
0.32	1.07	1.07	1.07
0.40	1.00	1.01	1.00
0.48	1.07	1.07	1.07
0.56	1.54	1.55	1.55
0.64	1.54	1.57	1.55
0.72	1.08	1.11	1.09
0.80	1.05	1.11	1.08
0.84	1.11	1.21	1.16
0.88	1.21	1.31	1.27
0.92	1.24	1.08	1.15
0.96	0.83	0.54	0.66
1.00	0.52	0.33	0.43

Table 4 Normalized displacement u

	$x=0$			$x=0.04b$		
			No. of terms			
y/b	30	35	40	30	35	40
0.80	0.93	0.99	1.00	0.94	0.98	1.00
0.84	0.95	0.98	1.01	0.94	0.99	1.01
0.88	0.94	0.97	1.01	0.94	1.00	1.01
0.92	0.90	1.02	1.00	0.94	1.05	1.04
0.96	1.03	1.19	1.17	1.01	1.14	1.13
1.00	1.09	1.21	1.20	1.06	1.17	1.16

Table 5 Normalized displacement u along $x=0.04b$

	No. of terms			
y/b	30	35	40	45
0.88	0.89	0.97	1.00	1.01
0.92	0.77	0.88	0.93	0.92
0.96	0.66	0.74	0.79	0.76

considered in the study, the convergence of the general solutions is first examined at locations close but not at the fastener line or the crack plane. Once the convergence of the general solutions is assured, the displacements at nodal points corresponding to a ten-node crack-tip element[11] are taken for the determination of the stress intensity factor. To examine the behavior and the convergence characteristics of the general solutions of the present analysis, a splice joint without a crack is considered. For the uncracked case, it is only necessary to consider a typical portion containing one fastener. The convergence of the dominant stress σ_x in the main sheet of region 4 along a line at $0.2b$ distance from the fastener line is shown in Table 1. Results shown in Table 1 are the longitudinal stresses normalized with respect to the stress at $x=0.2b$ and $y=0$ based on the 10-term solution. It may be noted that results based on a 12-term solution not shown in Table 1 are identical to the 10-term results.

While the 8-term solution is sufficiently accurate for the results shown in Table 1, the stress along the fastener line $x=0$ based on eight terms show significant discrepancies from that of a 10-term solution as shown in Table 2. However, one should note that the discrepancies in the longitudinal displacement, as shown in Table 2, are substantially smaller, or much less significant. Again, σ_x and the longitudinal displacement u are normalized with respect to their corresponding quantities at $x=0$ and $y=0$ based on the 10-term solutions. The results for σ_x computed along lines at distances larger than $0.4b$ from the fastener line based on a five-term approximation are found to be identical to those based on the eight or more term solutions. For this uncracked case, approximately ½ s of CPU time on a UNIVAC 1100/81 is needed to make a computer run.

Examples

In the subsequent examples for illustrative purposes, the Poisson's ratio $\nu=0.3$ will be used. As the first example, a splice joint containing five equally spaced fasteners with a $0.16b$ length crack located between $y=0.92b$ and $1.08b$ is considered. The stress σ_x along the line at a distance of $0.08b$ from the fastener line was examined. Results based on 30-, 35-, and 40-term approximations are given in Table 3, and the results are normalized with respect to σ_x at $x=0.08b$ and $y=0$ based on the 40-term solution. It is clear from Table 3 that σ_x converges very well except perhaps for values below the dotted line that correspond to the stress at locations adjacent to the crack. This shows that the general solution definitely converges. Furthermore, in the general region adjacent to the crack, and even along the crack line, the longitudinal displacement u is still very well behaved. The results for u normalized with respect to 40-term solution of displacement at $y=0.8b$ for $0.8b \le y \le b$ along $x=0$ and $0.04b$ where the nodal points of a potentially smallest crack-tip element may be located are given in Table 4.

For a $0.08b \times 0.08b$ crack-tip element, the longitudinal displacement u at node points located in region 3 at $0.04b$ distance from the fastener line is shown in Table 5 in which all results are normalized with respect to the displacement at $y=0.88b$ based on the 40-term solution, and good convergence may be noted.

Based on the results shown in Tables 4 and 5, the 40-term solution is sufficiently adequate. The fastener loads based on the 40-term solution are found to be

$$\bar{P}_1=\bar{P}_5=1.075, \quad \bar{Q}_1=-\bar{Q}_5=0.0018$$

$$\bar{P}_2=\bar{P}_4=1.122, \quad \bar{Q}_2=-\bar{Q}_4=0.0128$$

$$\bar{P}_3=0.606, \quad \bar{Q}_3=0.0000$$

where $\bar{P}_i=5P_i/2Nb$ and $\bar{Q}_i=5Q_i/2Nb$. If no crack occurs, $\bar{P}_i$ and $\bar{Q}_i$ should be 1 and 0, respectively. For this example problem, approximately 3 s of CPU time are used for each computer run.

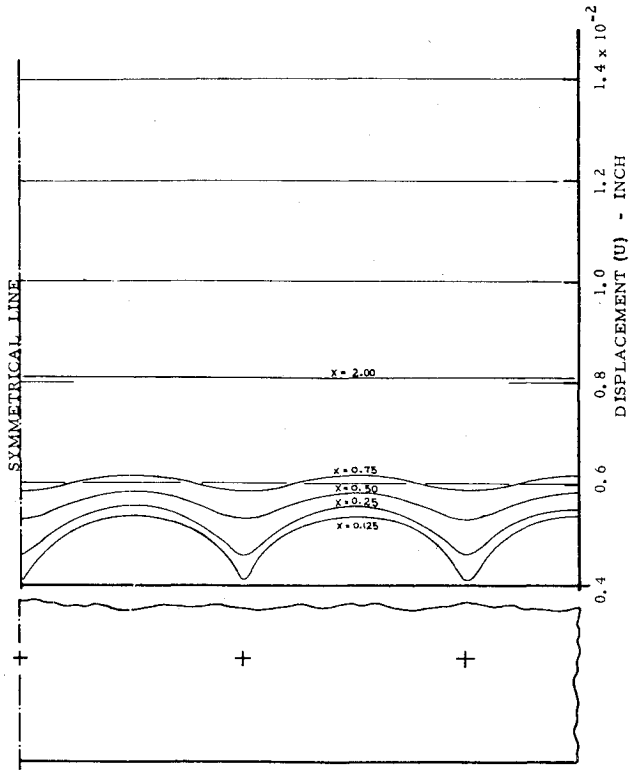

Fig. 3 Longitudinal displacement (without crack).

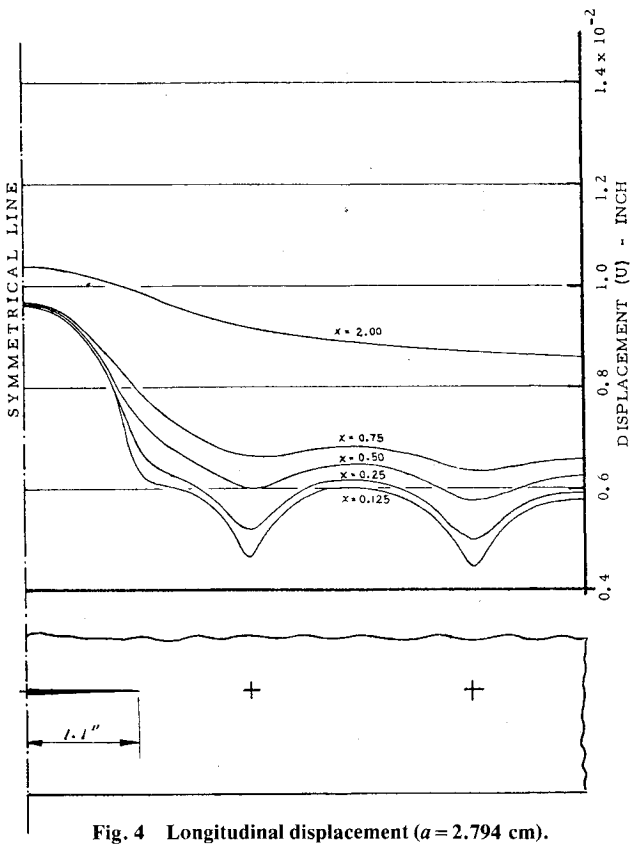

Fig. 4 Longitudinal displacement ($a = 2.794$ cm).

As a second example, a panel subjected to a uniform far-field stress $f_t = 132.59$ MPa (19.23 ksi) is considered. The fastener spacing is 5.588 cm (2.2 in.). Panel cracks of various lengths were assumed to occur symmetrically about a centrally located fastener as shown in Fig. 4 or 5. The longitudinal displacement at various locations of the main sheet without a crack is plotted in Fig. 3 which shows the periodic nature of the displacements. The corresponding displacements for the case with a half crack length of 2.794 cm (1.1 in.) are shown

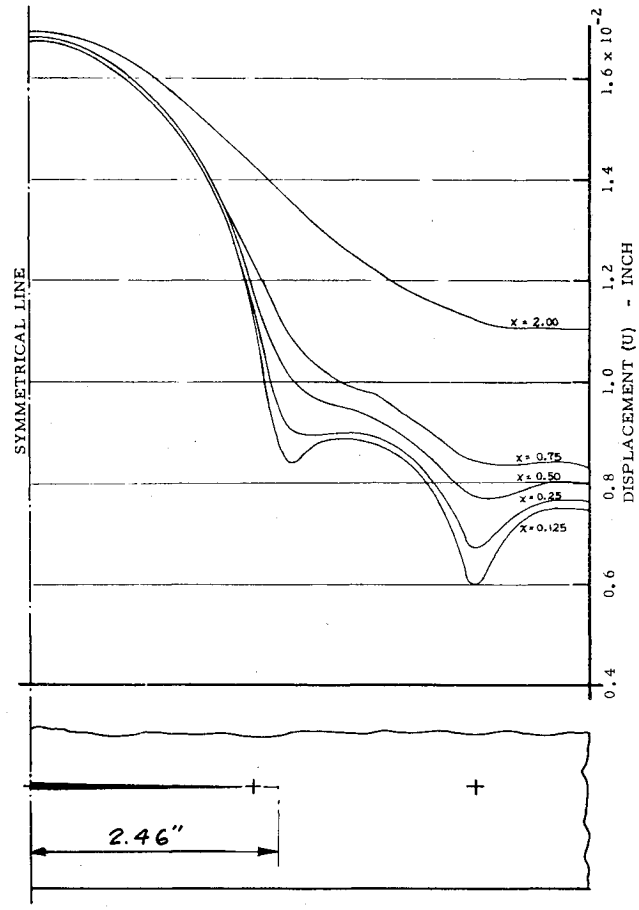

Fig. 5 Longitudinal displacement ($a = 6.2484$ cm).

Table 6 Stress-intensity factor/$\bar{K}$

Crack-tip element size, cm, (in.)	No. of terms 10	20	30	40
1.016×1.016 (0.4×0.4)	0	1.17	1.00	1.02
2.032×2.032 (0.8×0.8)	0.25	1.03	0.97	1.00
3.048×3.048 (1.2×1.2)	0.38	0.98	0.96	0.99

in Fig. 4. It is seen from Figs. 3 and 4 that the displacements in the cracked panel approach those in the uncracked panel at distance away from the cracked location. The displacements of a panel having a longer crack with 6.2484 cm (2.46 in.) half length are shown in Fig. 5. For this second example problem, results of the stress intensity factor corresponding to various number of term approximations for three different sizes of the crack-tip elements are given in Table 6 in which rapid convergence is evident. The crack length used was 5.588 cm (2.2 in.), and the panel width containing nine fasteners was used in the computation. The results shown in Table 6 are normalized with respect to the stress-intensity factor $\bar{K} = 30.36$ MPa$\sqrt{\text{m}}$ (27.63 ksi$\sqrt{\text{in.}}$) corresponding to the 2.032×2.032-cm (0.8×0.8-in.) crack-tip element size based on the 40-term solution.

For this example problem, approximately 6.5 s of CPU time is needed to make a computer run for the general analysis of the problem, and 1.2 s are used to subsequently compute the stress intensity factor using the crack-tip element. The variation in fastener loads P_i and normalized stress-intensity factors λ as a function of various crack lengths are plotted in Fig. 6. It is seen from Fig. 6 that the fastener load P_4 at the crack location decreases sharply as the crack length increases

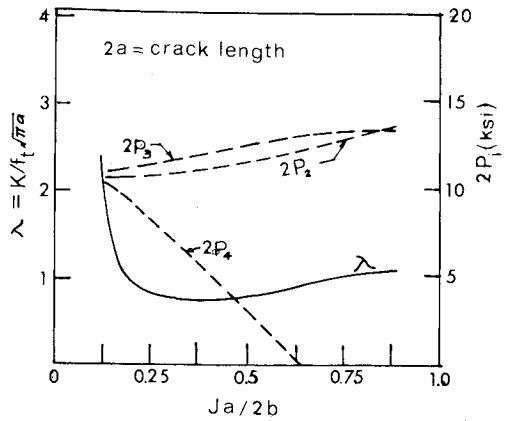

Fig. 6 Stress-intensity factor and fastener loads.

and that the adjacent fasteners pick up additional load in the process.

Concluding Remarks

The present work demonstrates that the analysis procedure established provides rapid and accurate determination of stresses and displacements including regions near the crack location. It has also been shown that results obtained by using the general analysis in conjunction with a high-order crack-tip element with ten nodal points can determine the stress intensity factor effectively. It appears, therefore, that to use this analysis procedure containing a crack-tip element is more desirable than using other numerical procedures.

References

[1] Wang, J.T.S. and Hsu, T. M., "Analysis of a Partially Cracked Panel," *Journal of Aircraft*, Vol. 9, July 1972, p. 503.

[2] Wang, J.T.S., Chu, J.C.S., Freyre, O., and Hsu, T. M., "Analysis of a Spliced Joint Containing a Crack," *Proceedings of the Fifth Canadian Congress of Applied Mechanics*, Fredericton, May 26-30, 1975, p. 155.

[3] Freyre, O. L., Lassiter, L. W., Aberson, J. A., and McKinney, J. M., "Application of Damage Tolerance Criteria to Multi-Plank Wing Cover Design," *Fracture Prevention and Control*, American Society of Metals, 1974, pp. 397-434.

[4] Swift, T., "The Effects of Fastener Flexibility and Stiffener Geometry on the Stress Intensity in Stiffened Cracked Sheets," *Proceedings of an International Conference on Prospects of Fracture Mechanics*, edited by G. C. Sih, H. C. Van Elst, and D. Brock, Delft University of Technology, The Netherlands, June 1974, pp. 389-404.

[5] Swift, T., "Development of the Fail-Safe Features of the DC-10," *Damage Tolerance in Aircraft Structures*, American Society for Testing and Materials, STP486, 1971, pp. 164-214.

[6] Ratwani, M. M. and Wilhem, D. P., "Development and Evaluation of Methods of Plane Stress Fracture Analysis—A Technique for Predicting Residual Strength of Structure," AFFDL-TR-73-42, Pt. II, Vol. I, April 1975.

[7] Bowie, O. L., "Analysis of Infinite Plate Containing Radial Cracks Originating from a Circular Hole," *Journal of Mathematics and Physics*, Vol. 23, April 1956, pp. 60-71.

[8] Sokolnikoff, I. S., *Mathematical Theory of Elasticity*, McGraw-Hill Book Company, New York, 1956.

[9] Timoshenko, S. and Goodier, J. N., *Theory of Elasticity*, McGraw-Hill Book Company, New York, 1951.

[10] Wang, C. T., *Applied Elasticity*, McGraw-Hill Book Company, New York, 1953.

[11] Aberson, J. A. and Anderson, J. M., "Cracked Finite-Element Proposed for NASTRAN," *NASTRAN User's Colloquium*, NASA TMX-2893, 1973, pp. 531-550.